

Supplementary information

Local Networks of Electrical Conductance in Hybrid Gold Nanoparticle-Polymer Films

Sukanya Das¹, Michael A.H. Klos^{1,2}, Tobias Kraus^{1,2}, Roland Bennewitz^{1,3*}

¹INM–Leibniz-Institute for New Materials, 66123 Saarbrücken, Germany

²Colloid and Interface Chemistry, Saarland University, 66123 Saarbrücken, Germany

³Department of Physics, Saarland University, 66123 Saarbrücken, Germany

**Email: roland.bennewitz@leibniz-inm.de*

Contents

1. Surface features of AuNPs@PEDOT:PSS/PVA films recorded in tapping mode AFM..	2
Ink-jet printed films of high concentration ink.....	2
Drop-casted films of low-concentration ink	3
2. Negligible variation of current magnitudes across individual AuNPs	4
3. Contact mode current images from high concentrated ink surfaces	5
4. Details of resistance difference maps	6
5. Disconnected clusters of particles.....	7
6. Tip degradation and evolution of current maps in continuous scanning	8
7. Contact mode current images from low concentration ink surfaces without PVA ...	10

1. Surface features of AuNPs@PEDOT:PSS/PVA films recorded in tapping mode AFM

Ink-jet printed bulk films produced with high-concentration ink

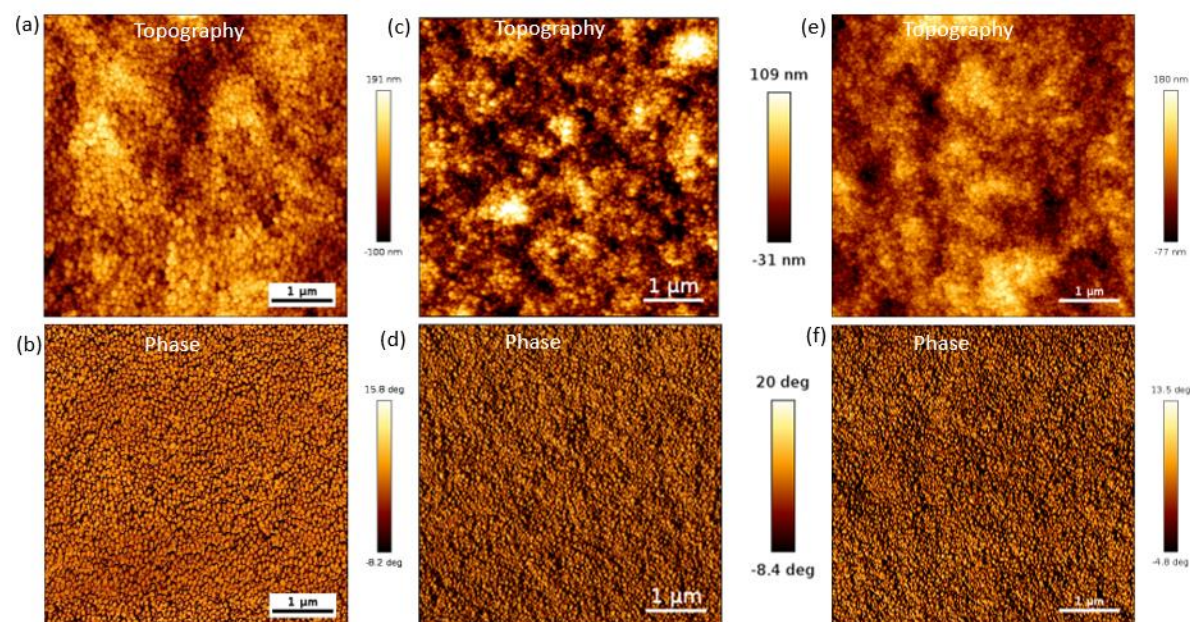


Figure S1. a) Tapping mode maps of (a,c,e) topography and (b,d,f) phase ($5 \times 5 \mu\text{m}^2$).

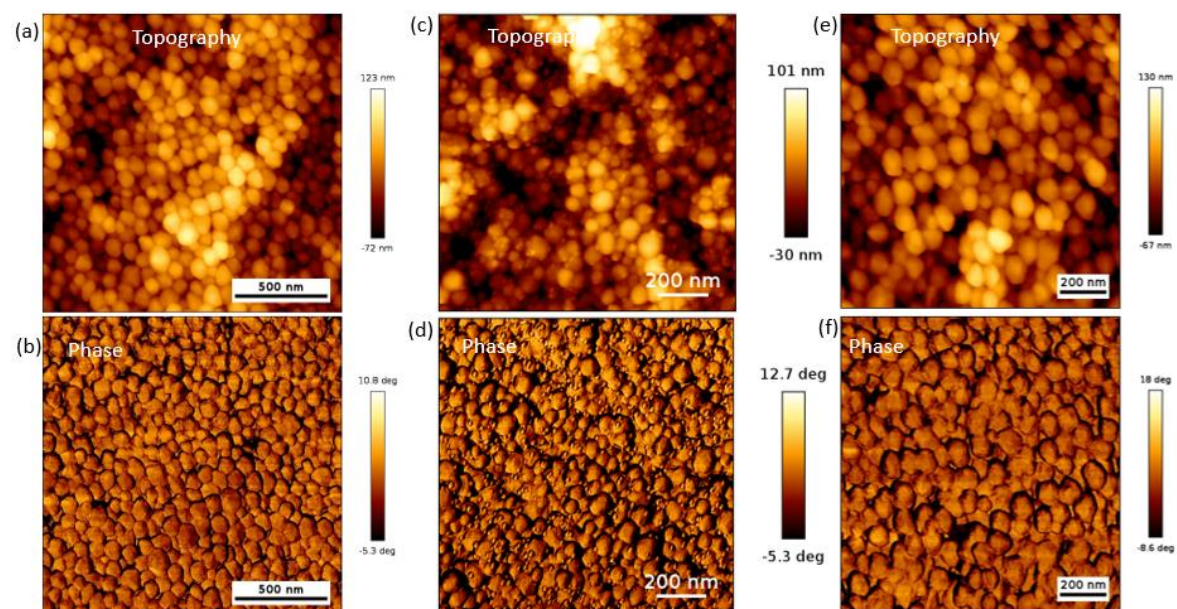


Figure S1. b) Tapping mode topography and phase maps of an area of (a,b) $2 \times 2 \mu\text{m}^2$, (c,d) $1.2 \times 1.2 \mu\text{m}^2$, (e,f) $1.2 \times 1.2 \mu\text{m}^2$.

Few-layer films produced by drop casting low-concentration ink

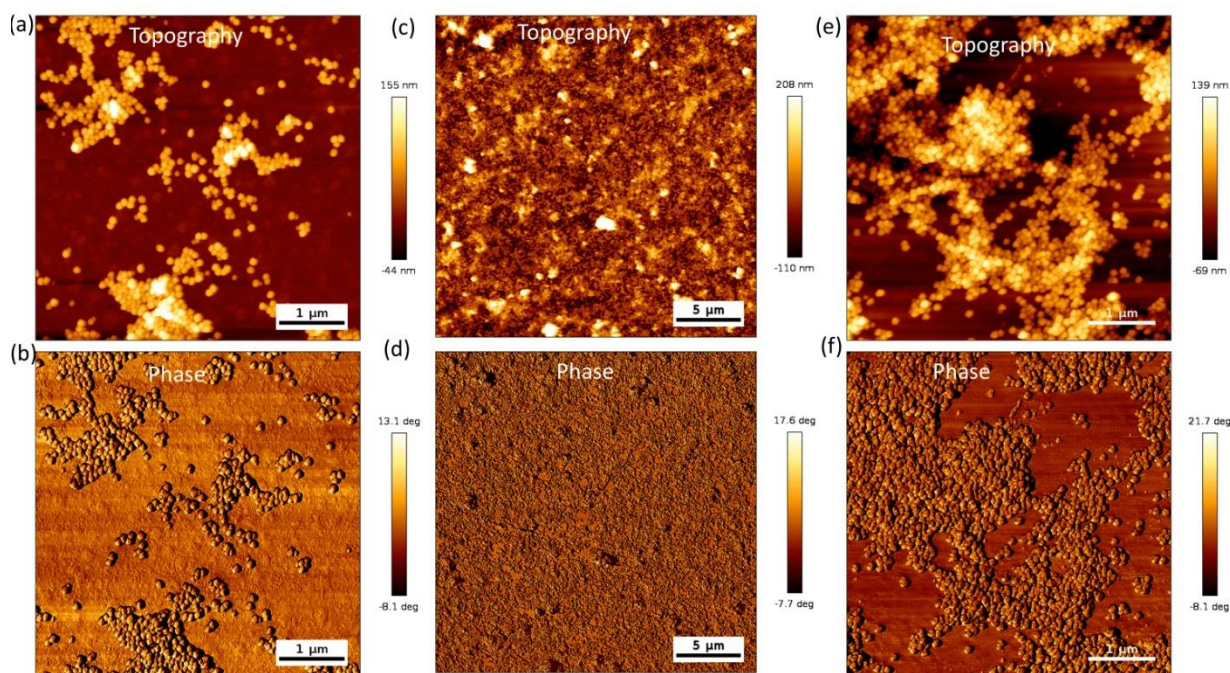


Figure S1. c) Tapping mode topography and phase maps of an area of (a,b) 5x5 μm^2 , (c,d) 25 x 25 μm^2 , (e,f) 5 x 5 μm^2 .

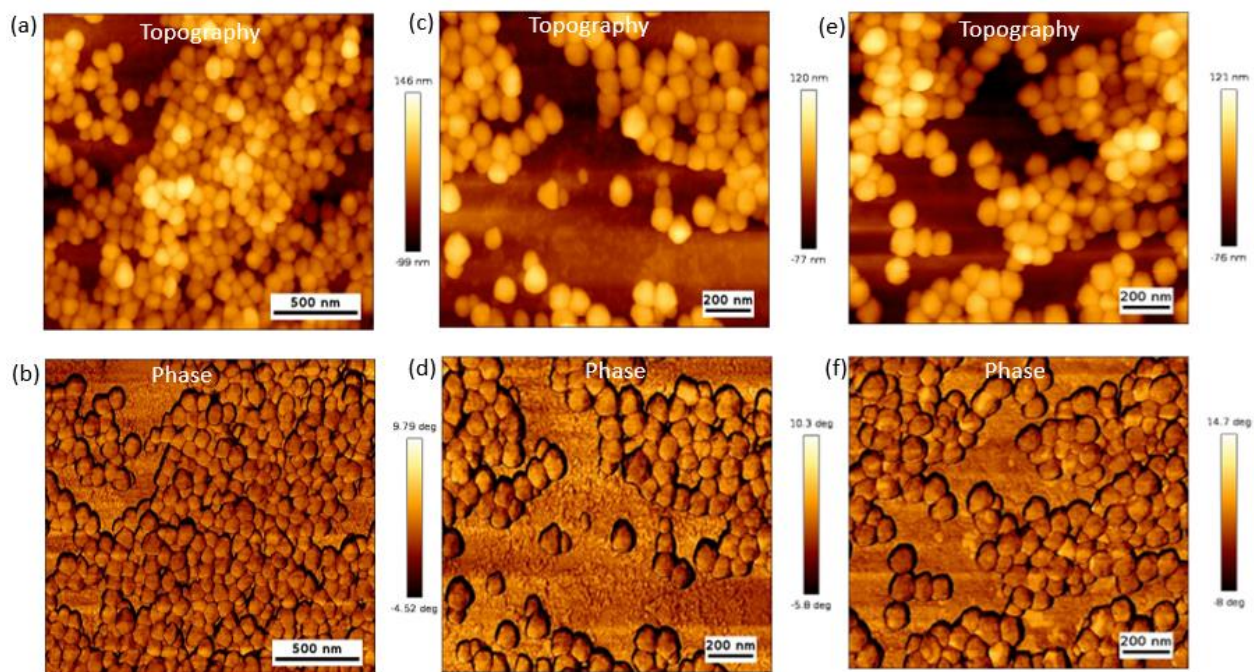


Figure S1. d) Tapping mode topography and phase maps of an area of (a,b) 1.98 x 1.98 μm^2 , (c,d) 1.4 x 1.4 μm^2 and (e,f) 1.4 x 1.2 μm^2 .

The bulk films in Figure S1a,b show the surface of a $\sim 1\ \mu\text{m}$ thick layer of dense nanoparticles, while the few-layer films in Figure S1 c,d show a thin layer of only few or single layers of nanoparticles on the substrates.

2. Negligible variation of current magnitudes across individual AuNPs

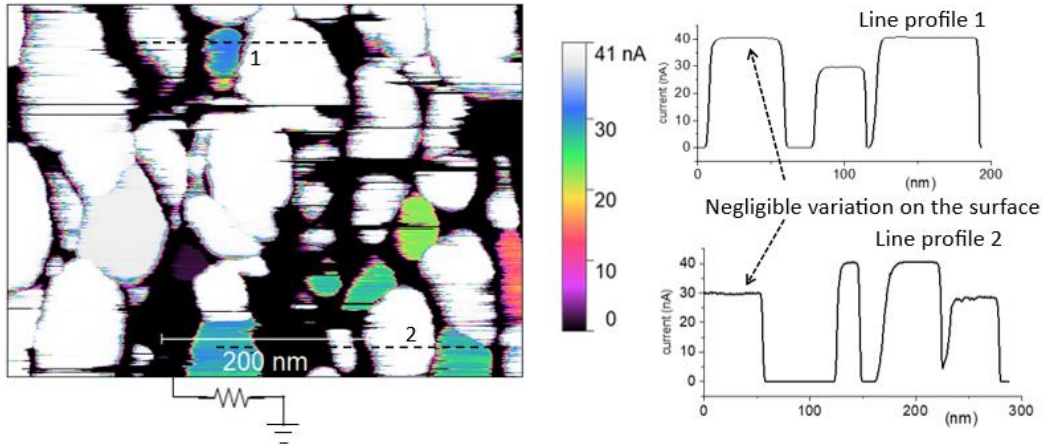


Figure S2. Current map recorded by cAFM on a bulk film, measured with a high-ohmic series resistor. The current map shows negligible variations of current across the area of each nanoparticle. The constant current at different levels confirms that the contact resistance between the tip and the nanoparticles is negligible compared to the resistance between the particles and the underlying conductive network.

3. Contact mode current images of bulk films

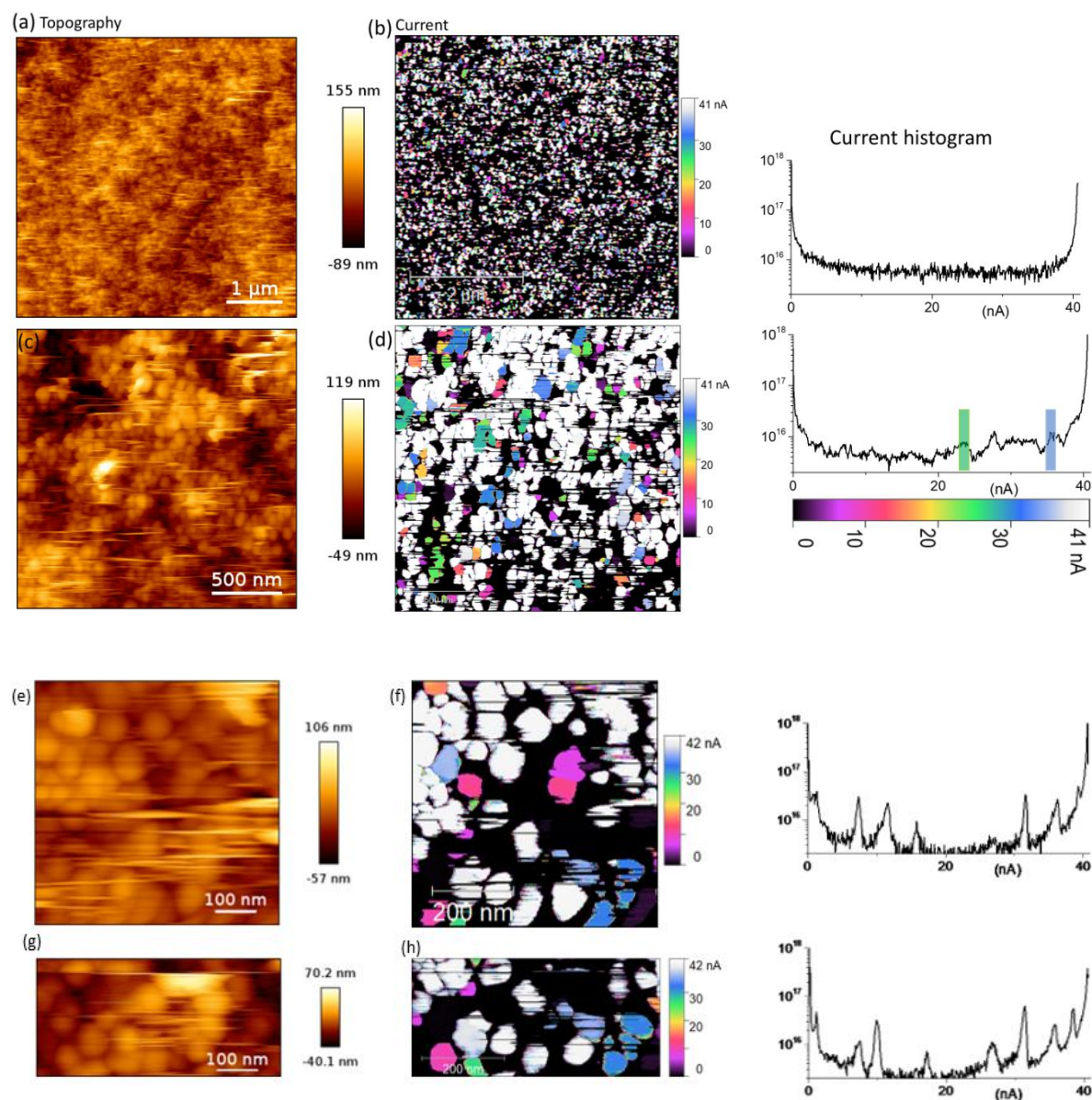


Figure S3. Conductive AFM on bulk film surfaces. (a,c,e) Topography maps and (b,d,f) corresponding current maps, recorded over a surface area of $5\ \mu\text{m} \times 5\ \mu\text{m}$, $2\ \mu\text{m} \times 2\ \mu\text{m}$ and $600\ \text{nm} \times 600\ \text{nm}$, respectively. (g,h) are the topography and current maps of the second scan on the lower half of (e), where the same configuration of nanoparticles and the same current magnitudes can be recognized. The right column displays corresponding current histograms. The area marked green and blue in the histogram for reference represents their respective distinct colored regions in the current map.

4. Details of resistance difference maps

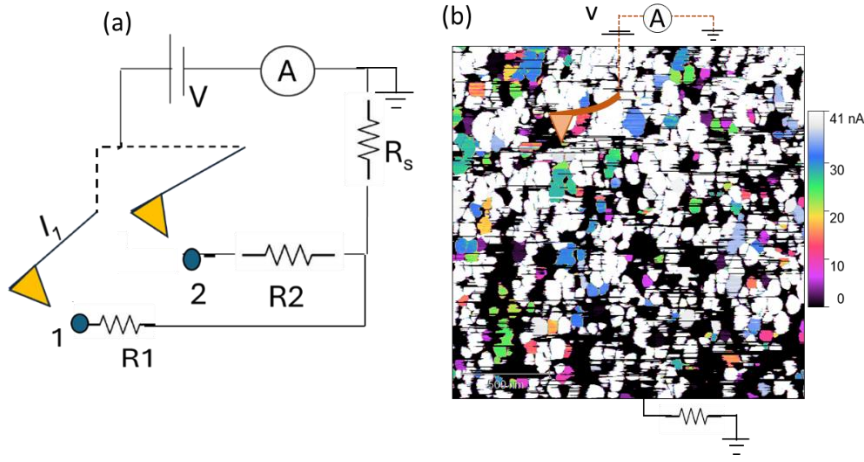


Figure S4. (a) Equivalent circuit of the cAFM with the hybrid ink surface (b) for determination of the resistance difference between two points 1,2.

Let point 1 and 2 be any points on the sample surface in Figure S4 where the cAFM tip contacts during the scan and V_{appl} is the applied bias voltage. In our analysis we chose I_2 to be the highest current in a given current map as reference point 2 for current flowing through the circuit into the surface area of this scan. We then calculate the resistance difference for each point 1 in the map with respect to reference point 2 as:

$$\Delta R = R_1 - R_2 = \left(\frac{V_{appl}}{I_1} - R_s \right) - \left(\frac{V_{appl}}{I_2} - R_s \right) = V_{appl} \left(\frac{1}{I_1} - \frac{1}{I_2} \right) = V_{appl} \frac{I_2 - I_1}{I_2 I_1}$$

5. Disconnected clusters of particles

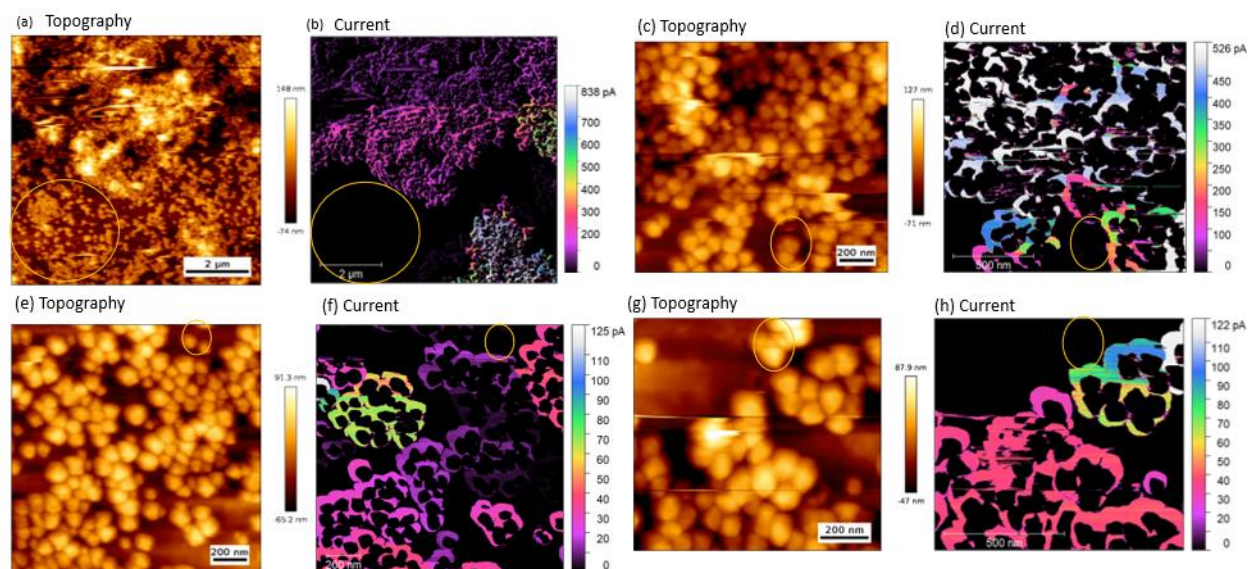
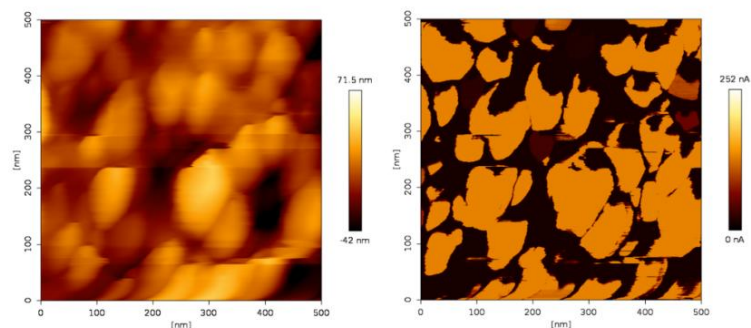


Figure S5. Examples for clusters of particles (encircled), which are observed in the topography maps, but do not show any signal in the simultaneously recorded current map. Images were recorded on different areas of few-layer films.

6. Tip degradation and evolution of current maps in continuous scanning

First scan:



Second scan of the same area:

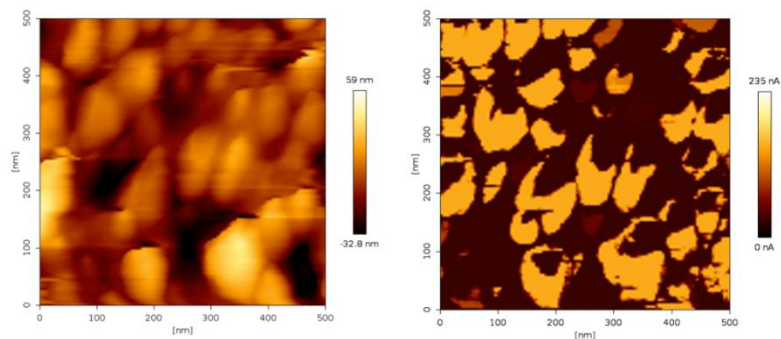


Figure S6a: Current maps from subsequent scans of the same area on a bulk film. The spots of zero current in the center of each particle grow from the first to the second scan. Please note that the relative position of each nanoparticle is shifted between the first and second scan due to instrumental drift in this initial phase of imaging a new area.

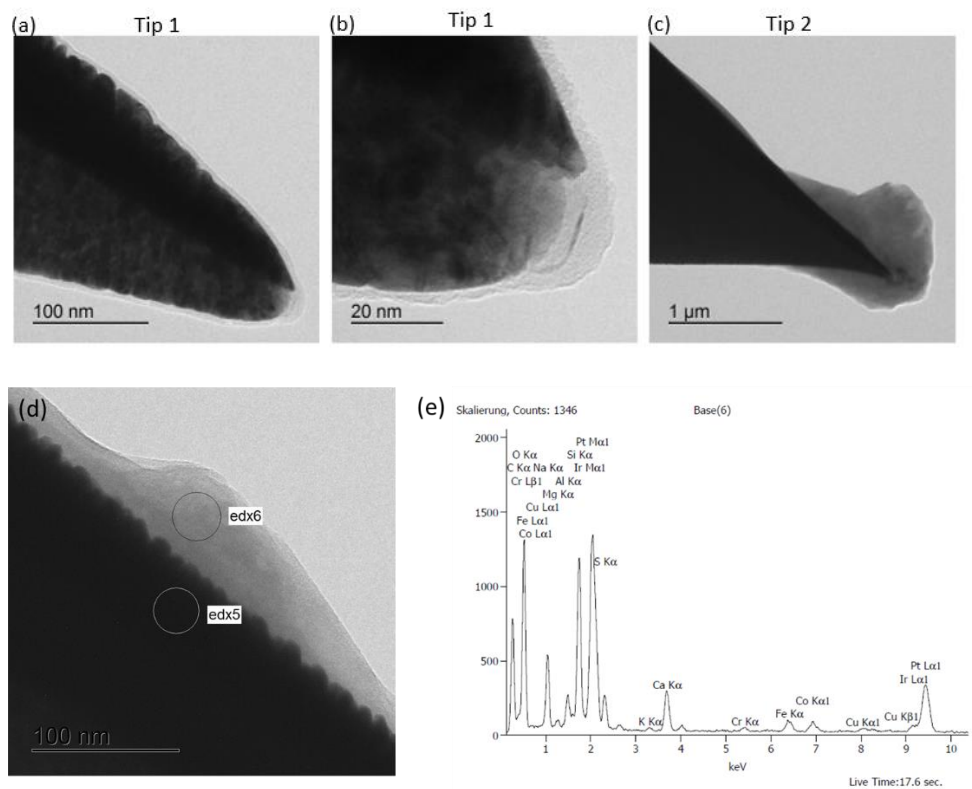


Figure S6b. (a-c) Transmission Electron Microscopy images of two tips used for cAFM on hybrid ink surfaces (JEOL 2100, beam current: 60 pA/cm²). (e) Energy-dispersive X-ray (EDX) analysis at spot 6 of tip 1 (d). The sulfur count in the EDX spectrum recorded at spot 6 indicates the presence of polymer on the tip.

7. Contact mode current images of few-layer films produced from low-concentration inks without PVA

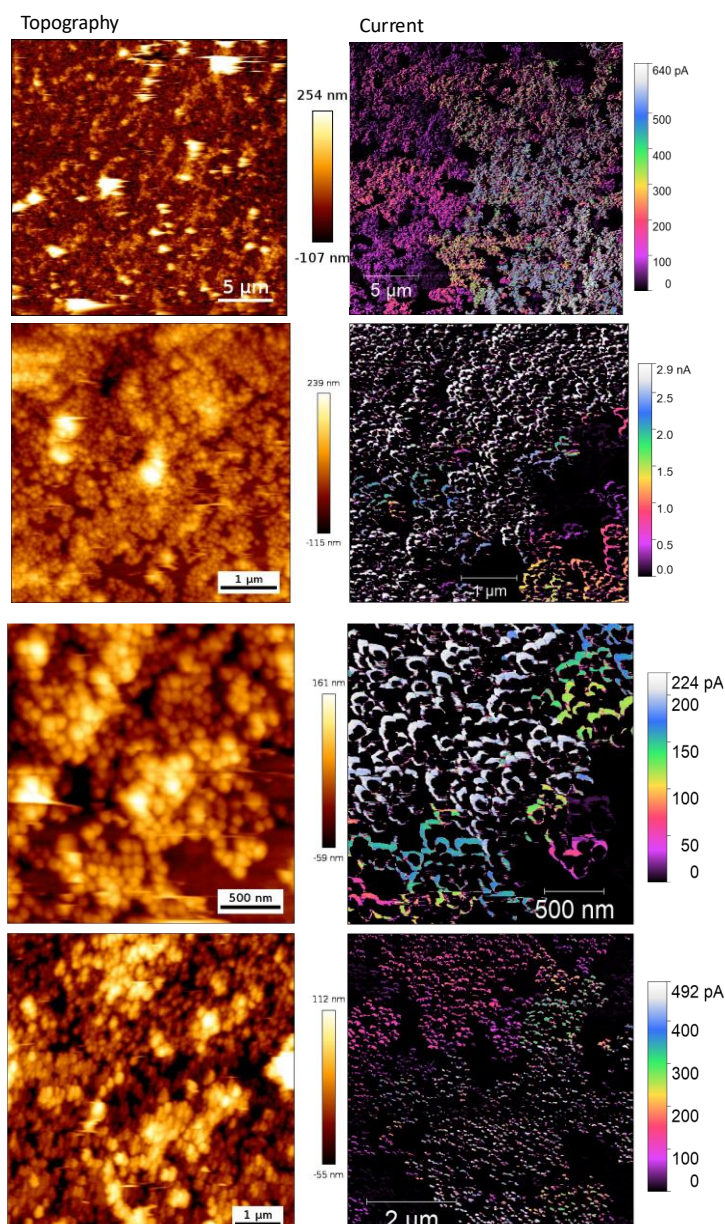


Figure S7. Topography and corresponding current maps recorded by cAFM at a bias of 1.2 V on drop-casted films of low-concentration ink without any added PVA. The presence of distinct regions of equal current is the same as on the films produced from ink containing PVA.

These examples confirm that the high resistance between particles or clusters of particles is characteristic to the hybrid nanoparticles and not induced by the addition of PVA.